2016

Biofilm growth kinetics and nutrient (N/P) adsorption in an urban lake using reclaimed water: A quantitative baseline for ecological health assessment

Tianzhi Wang

Zhenci Wu

Yunkai Li

See next page for additional authors

Funder: National Natural Science Fund of China; Key Project of the Beijing Eleventh-Five Year Research Program; Department of Water Resources; Special Fund for Water Conservancy Scientific Research in the Public Interest

Authors

Tianzhi Wang, Zhenci Wu, Yunkai Li, Mingchao Liang, Zhenhua Wang, and Paul Hynds

Biofilm growth kinetics and nutrient (N/P) adsorption in an urban lake using reclaimed water: A quantitative baseline for ecological health assessment

Article *in* Ecological Indicators · December 2016

DOI: 10.1016/j.ecolind.2016.07.046

CITATIONS
7

READS
88

6 authors, including:

Tianzhi Wang
Tianjin University
18 PUBLICATIONS **119** CITATIONS
SEE PROFILE

Zhenci Xu
The University of Hong Kong
39 PUBLICATIONS **1,083** CITATIONS
SEE PROFILE

Yunkai Li
China Agricultural University
160 PUBLICATIONS **2,083** CITATIONS
SEE PROFILE

Zhenhua Wang
shihezi university
59 PUBLICATIONS **487** CITATIONS
SEE PROFILE

Elsevier Editorial System(tm) for Ecological Indicators

Manuscript Draft

Manuscript Number: ECOLIND-6466R1

Title: Biofilm Growth Kinetics and Nutrient (N/P) Adsorption in an Urban Lake using Reclaimed Water: A Quantitative Baseline for Ecological Health Assessment

Article Type: Research paper

Keywords: Biofilms; Reclaimed water; Lake; Growth kinetics; Nutrient Adsorption, Eutrophication, Ecological Health Assessment

Corresponding Author: Dr. Paul Hynds,

Corresponding Author's Institution: Dublin Institute of Technology

First Author: Tianzhi Wang

Order of Authors: Tianzhi Wang; Zhenci Xu; Yunkai Li; Mingchao Liang; Zenhua Wang; Paul Hynds

Abstract: Reclaimed wastewater reuse represents an effective method for partial resolution of increasing urban water shortages; however, reclaimed water may be characterized by significant contaminant loading, potentially affecting receiving ecosystem (and potentially human) health. The current study examined biofilm growth and nutrient adsorption in Olympic Lake (Beijing), the largest artificial urban lake in the world supplied exclusively by reclaimed wastewater. Findings indicate that solid particulate, extracellular polymeric substance (EPS) and metal oxide (Al, Fe, Mn) constituent masses adhere to a bacterial growth curve during biofilm formation and growth. Peak values were observed after ≈30 days, arrived at dynamic stability after ≈50 days and were affected by growth matrix surface roughness. These findings may be used to inform biofilm cultivation times for future biomonitoring. Increased growth matrix surface roughness (10.0μm) was associated with more rapid biofilm growth and therefore an increased sensitivity to ecological variation in reclaimed water. Reclaimed water was found to significantly inhibit biofilm nutrient adsorption when compared with a "natural water" background, with elevated levels of metal oxides (Al, Fe, and Mn) and EPS representing the key substances actively influencing biofilm nutrient adsorption in reclaimed water. Results from the current study may be used to provide a quantitative baseline for future studies seeking to assess ecosystem health via monitoring of biofilms in the presence of reclaimed water through an improved quantitative understanding of biofilm kinetics in these conditions.

Response to Reviewers: The authors are very grateful to the reviewers for improving our manuscript. All author responses are included in the author response document

ECOLIND-6466

Reviewer Comments & Author Responses

Reviewer 1, Comment: *You correctly started by stating that freshwater resources are increasingly falling behind ever-increasing consumption which is fuelled by rapid urbanization, economic growth etc. At this point, you may like to give some descriptive statistics regarding freshwater consumption and freshwater capacity in China and/or in Beijing region.*

Author Response: *The authors agree that the recommended addition would be helpful for the audience to place the current work in a national and global context. Accordingly, the following paragraph has been added to the manuscript:*

Recent studies have specifically highlighted Beijing as an urban area characterised by sever water resource pressures (Zhang et al., 2011; Gao et al., 2014). For example, Jenerette et al. (2006) estimate that while Beijing requires approximately 3064 ML/day, locally available resources account for only a fraction of this, necessitating significant water imports from neighbouring Hebei. Moreover, calculations indicate a total annual water footprint of approximately 47 x 10^8 m^3/annum, equating to an individual water footprint of 648 m^3/annum, which is significantly higher to the national mean of 391 m^3/annum (Zhao et al., 2009; Ge et al., 2011). During the 4-year period 2011-2014, freshwater consumption in Beijing outstripped local freshwater resources by 39.3% (Beijing Water Authority, 2015).

Reviewer 1, Comment: *if the article is accepted and printed in black and white, some of your Figures (i.e. Figures 1,2,3) will become untrackable. You may like to redraw the lines with different markers and line types so as to differentiate different series.*

Author Response: The authors agreed that Figures 1-3 (now Figures 2-4 due to addition of supplementary Figure 1) would not be readable in grayscale. Accordingly, we have followed the reviewers recommendation by amending these figures to black/white/grayscale. We have chosen not to amend Figure 5 (Previously Figure 4), as this figure is readable in its current format when viewed in grayscale.

Reviewer 2, Comment: While the very sophisticated mathematical and statistical approach employed is in my opinion completely correct and sound, I think that it is not clearly explained to the common reader. This section could be more clearly presented, the variables and equations perhaps presented in boxes or tables, and not directly "embedded" along the text. Otherwise, its okay. All information required is presented.

Author Response: *The authors agree that the overall mathematical/statistical approach used required additional presentation. We have chosen to leave equations embedded within the text in order that more mathematically minded reader have adequate detail for study replication. However, we have developed and added a new Figure 1, as follows to help simplify the overall modelling approach for readers. All other figure numbers and titles have been amended accordingly.*

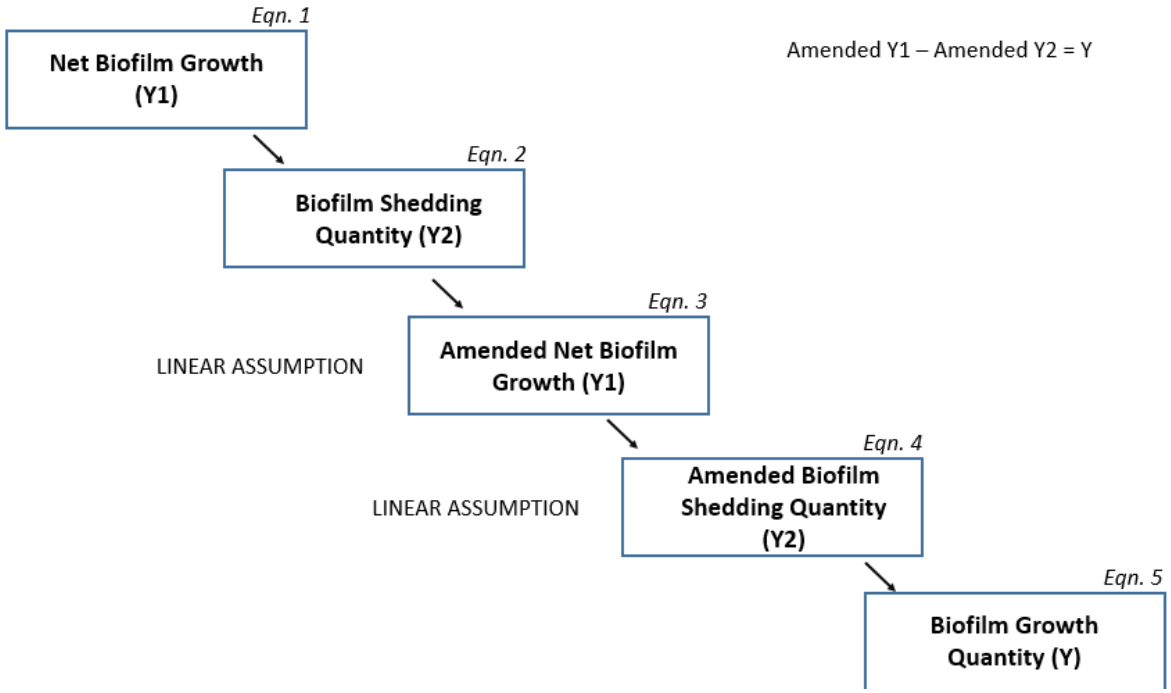

Figure 1. Schematic outlining the employed biofilm growth kinetic model

Reviewer 2, Comment: *There are two references in the list cited in the text as "Wang et al, 2013a" and "Wang et al, 2013b) that are properly quoted. However, twice the quotation "Wang et al, 2013" is present in the text. This should be fixed.*

Author Response: *Thank you for pointing this mistake out. Accordingly, we have corrected the error; both are now Wang et al., 2013a*

Reviewer 2, Comment: *The reference "Wang et al, 2010" was quoted in the text but not listed.*

Author Response: *This was a mistake on the authors part; thank you for pointing it out. We have amended it to Wang et al., 2013a*

Reviewer 2, Comment: *The reference "Oliveira et al, 2014" was quoted in the text also but not listed (Mistyping? Olivieri et al, 2014?)*

Author Response: *Yes, the reviewer is absolutely correct, this was a mis-spelling. We have amended to read Olivieri et al, 2014*

Reviewer 2, Comment: *Two different algorithms were mentioned, LM and ME. I figured this as typing error. If this is not the case, this point should be made clear in the text. In the other hand, calibration results were very good.*

Author Response: *Yes, the reviewer is correct, only one iterative algorithm was used, namely the Levenberg-Marquardt (LM) algorithm; accordingly, the text has been amended from ME to LM*

Reviewer 2, Comment: As indicated by the authors along the text, biofilms are formed by complex inorganic/organic mixtures of substances from different origins and having different properties. Thinking about the measurements of biofilms properties presented in this work, and with the background measurements presented in the reservoir water (Table 1), no conclusion can be drawn about the "health" of an artificial ecosystem at least as I can guess what this health could mean: the capacity of this closed or semi-closed system to support different forms of life, to support some form of food production, or to provide water resources for human use.
In my opinion the authors would benefit from being less emphatic in their conclusions and by pointing out the limitations of this kind of study on ecosystem health evaluation. From this aspect, I think they are very far off the mark.

Author Response: *The authors agree that the original manuscript was perhaps too emphatic with respect to the discussion and conclusions section, and that the presented study, while useful and novel, did not provide sufficient data to make definite conclusions with respect to the use of biofilms as effective ecological monitors. Accordingly, the authors have made the following manuscript amendments:*

Methods Section: *The following sentence has been added:*

According to Gan & Bai (2010), both treatment plants achieve ≈ 6-log virus and bacteria removal, 3-log turbidity removal, ≥91% removal of linear alkylbenzene sulfonates (LAS), and ≥98% removal of volatile phenols.

Discussion Section: *Overall, we have tempered the language throughout the discussion to correctly reflect the study findings and not overemphasize or overstate the conclusions which may confidently be drawn from the collated data. Additionally, the following paragraph have been added:*

It is important to note that, within the context of ecosystem health assessment, the current study comprised some inherent limitations, instead focusing on biofilm growth kinetics in a reclaimed wastewater background. The current study did not include eco-toxicological analyses, and thus only indicative conclusions pertaining to ecological health may be made. Future work should concentrate on biofilm growth kinetics and responses to the presence of ecologically harmful compounds, in addition to human toxins and pathogens including heavy metals, PAHs, urban pesticides, and endocrine disruptors.

Conclusions Section: *The following paragraph has been added: Accordingly, it is concluded that biofilms may be effective indicators of ecological health in aquatic ecosystems characterized by the presence of reclaimed water i.e. indicators of system capacity to support food production and/or provide water resources for human use. However, significant further work is required to elucidate the association between biofilm presence and associated growth kinetics, and the human health related contaminants of primary concern e.g. PAHs, urban pesticides, endocrine disruptors, enteric pathogens, etc.*

Biofilm Growth Kinetics and Nutrient (N/P) Adsorption in an Urban Lake using Reclaimed Water: A Quantitative Baseline for Ecological Health Assessment

Wang Tianzhi[1], Xu Zhenci[1], Li Yunkai[1,*], Liang Mingchao[1], Wang Zhenhua[2], Paul Hynds[3]

[1] College of Water Resources and Civil Engineering, China Agricultural University, Beijing 100083, China

[2] College of Water and Architectural Engineering, Shihezi University, Shihezi City 832000, Xinjiang, China

[3] School of Civil and Structural Engineering, Dublin Institute of Technology, Bolton St., Dublin 7, Republic of Ireland

Abstract:

Reclaimed wastewater reuse represents an effective method for partial resolution of increasing urban water shortages; however, reclaimed water may be characterized by significant contaminant loading, potentially affecting receiving ecosystem (and potentially human) health. The current study examined biofilm growth and nutrient adsorption in Olympic Lake (Beijing), the largest artificial urban lake in the world supplied exclusively by reclaimed wastewater. Findings indicate that solid particulate, extracellular polymeric substance (EPS) and metal oxide (Al, Fe, Mn) constituent masses adhere to a bacterial growth curve during biofilm formation and growth. Peak values were observed after ≈30 days, arrived at dynamic stability after ≈50 days and were affected by growth matrix surface roughness. These findings may be used to inform biofilm

* ***Corresponding author*** Yunkai Li
Tel: 86-10-62738485; Fax: 86-10-62738485; E-mail address: liyunkai@126.com

cultivation times for future biomonitoring. Increased growth matrix surface roughness (10.0μm) was associated with more rapid biofilm growth and therefore an increased sensitivity to ecological variation in reclaimed water. Reclaimed water was found to significantly inhibit biofilm nutrient adsorption when compared with a "natural water" background, with elevated levels of metal oxides (Al, Fe, and Mn) and EPS representing the key substances actively influencing biofilm nutrient adsorption in reclaimed water. Results from the current study may be used to provide a quantitative baseline for future studies seeking to assess ecosystem health via monitoring of biofilms in the presence of reclaimed water through an improved quantitative understanding of biofilm kinetics in these conditions.

Keywords: Biofilms; Reclaimed water; Lake; Growth kinetics; Nutrient Adsorption, Eutrophication, Ecological Health Assessment

1. Introduction

Increasing socioeconomic development, urbanization and wastewater production, in concurrence with the predicted effects of climate change will have far reaching consequences for global aquatic ecosystems, particularly those situated within urban and peri-urban areas. Presently, an estimated 80% of global wastewater remains untreated and as such, is not reclaimed or reused; effective wastewater reuse serves the dual purpose of diversion from the aquatic environment and supplementary resource provision (Beaudequin *et al.*, 2015) and is therefore particularly beneficial in regions characterized by water scarcity and/or significant aquatic contamination.

Recent studies have specifically highlighted Beijing as an urban area characterized by sever water resource pressures (Gao & Hu, 2011; Zhang & Anadon, 2014). For example, Jenerette *et al*. (2006) estimate that while Beijing requires approximately 3064 ML/day, locally available resources account for only a fraction of this, necessitating significant water imports from neighboring Hebei. Moreover, calculations indicate a total annual water footprint of approximately 47 x 10^8 m^3/annum, equating to an individual water footprint of 648 m^3/annum, which is significantly higher to the national mean of 391 m^3/annum (Zhao *et al*., 2009; Ge *et al*., 2011). During the 4-year period 2011-2014, freshwater consumption in Beijing outstripped local freshwater resources by 39.3% (Beijing Water Authority, 2015). Numerous studies have reported high levels of support for water reuse among the general public, however, these studies have also shown that support decreases in line with increasing levels of human contact, leading to underutilization of reclaimed water for recreation and consumption (i.e. aquifer recharge) (Friedler *et al*., 2006). This has been further exacerbated by public health concerns resulting from the difficulties associated with pathogen detection and identification in reclaimed wastewater (Graczyk & Lucy, 2007; Olivieri *et al*., 2014).

Biofilms are composite systems primarily composed of photoautotrophic (algae) and heterotrophic (bacteria, fungi and protozoa) microorganisms, inorganic minerals and organic polymers which form semi-stable dynamic systems (Rao, 1997). These systems adhere to living or inanimate surfaces in multiple settings and are embedded within a self-produced matrix of extracellular polymeric substances (EPS),

a polymeric conglomeration comprising proteins, polysaccharides, nucleic acids, uronic acids, lipids, humic acids and amino acids, of which proteins and extracellular polysaccharides comprise 70–80% of the total (Hong & Herbert 2002; Hall-Stoodley *et al*., 2004; Lear & Lewis, 2012). The formation, growth and response of aquatic biofilms is closely connected with several physical, chemical and biological factors including water current, substrate type, growth surface, light, temperature, organic and inorganic chemical constituents (i.e. nutritional cues) and microbial composition (Lear & Lewis, 2012).

Ecological health assessment is a process by which the nature and effects of anthropogenic activities on the local environment are monitored and quantified for the purposes of future management and control (Porsbring, 2007). Monitoring may be undertaken via physical, chemical or biological techniques, with Porsbring (2007) maintaining that biological techniques via the use of naturally occurring native organisms (biomonitors) represent the most direct and effective monitoring approach within aquatic systems. Changes in aquatic biological communities often directly reflect physical, chemical and/or biological factors, in addition to the overall health of the ecosystem. Lear & Lewis (2009) have previously employed bacterial DNA fingerprint data from surface water streams to assess the impact of catchment landuse i.e. increasing urban development. Similarly, Rotter *et al*. (2013) report that periphyton levels in the River Elbe (a mixture of algae, cyanobacteria, heterotrophic microbes and detritus attached to aquatically submerged surfaces) may be used to provide an ecologically relevant assessment of pesticide effects under field conditions

for successful implementation of the EU Water Framework Directive (WFD).

Biofilms have been shown to both accurately and quickly reflect environmental variation, leading to their use as biomonitors and/or indices for aquatic ecosystem health evaluation (Eppley, 1977; Burns & Ryder, 2001; Guasch *et al*., 2003; Lawrence *et al*., 2004; Porsbring, 2007, Ancion *et al*., 2014). Yan *et al*. (2014) investigated the responses of freshwater biofilms to pollutants and overall ecosystem health in Baiyangdian Lake, China. Biofilm biomass production, chlorophyll production, extracellular enzyme activity and polysaccharide content were all measured in the context of pollutant exposure. Results indicate that biofilms provide salient information pertaining to contamination detection and ecological health assessment; biofilms associated with artificial substrata were recommended for future bio-monitoring at the site. Burns & Ryder (2001) and Lawrence *et al*. (2004) have previously shown the efficacy of using biofilms as bio-monitors in riverine systems. Due to the aforementioned lack of sustainable water supply in some regions and increasing global rates of urbanization, the utilization of reclaimed wastewater to supplement inland waterbodies represents an effective method for alleviation of urban water shortages. The inherently high levels of nitrogen, phosphorous and microorganisms present in reclaimed water frequently result in diverse and in some cases unique biofilm communities.

To date, few studies have focused on biofilm growth kinetics or contaminant absorption within aquatic environments supplied partly or wholly by reclaimed water. Those which have been undertaken indicate that the presence of biofilm is associated

111 with measureable levels of both nitrogen and phosphorus adsorption (Liang *et al*.,
112 2013; Wang et al., 2013a). In order to establish the potential efficacy of biofilms as
113 effective indicators of ecological health in aquatic ecosystems fed by reclaimed water,
114 it is critical that these processes are appropriately quantified.

115 The current study applied in-situ sample cultivation and laboratory analyses to
116 investigate biofilm growth kinetics and nutrient (nitrogen and phosphorus) adsorption
117 processes in Olympic Lake, Beijing. A growth model has been developed to elucidate
118 the growth kinetics of biofilms associated with an aquatic environment dominated by
119 reclaimed water. Dynamic variations of organic (EPS) and inorganic (Al, Fe, Mn)
120 biofilm constituents have been quantified, in addition to the solid particulate fraction.
121 Finally, three isotherm equations have been used to model the N and P adsorption
122 processes.

123

124 **2. Materials and Methods**

125 ***2.1 Study Site***

126 Olympic Lake is located in the Chaoyang district of Beijing and was constructed
127 in 2007 as the primary aquatic sports venue for the 29th Olympic Games. It has an
128 area of 165,000 m^2, a depth range of 0.6–1.1 m and a total volume of 159,000 m^3
129 (Wang *et al*. 2013a), thus making it the largest constructed aquatic system in the
130 world supplied entirely by reclaimed water. The lake is currently employed as an
131 urban artificial ecological water system, with two primary reclaimed water sources
132 employed, namely, the Qinghe Reclaimed Water Treatment Plant (80,000 m^3/d,

ANANOX (Anaerobic-Anoxic-OXic Process)) and the Beixiaohe Reclaimed Water Treatment Plant (60,000 m^3/d, Membrane Bioreactor + Reverse Osmosis). Based upon the current *Chinese Environmental Quality Standards for Surface Water* (GB 3838-2002), background water quality in the Olympic Green's central and northern areas are categorized as Levels III and IV, respectively. According to Gan & Bai (2010), both treatment plants achieve ≈6-log virus and bacteria removal, 3-log turbidity removal, ≥91% removal of linear alkylbenzene sulfonates (LAS), and ≥98% removal of volatile phenols. The variation in measured lake water chemistry during the 58-day biofilm sampling period is presented in Table 1.

2.2 Collection and Preparation of Biofilm Samples

Due to the ease with which glass slides may be processed to simulate variable surface matrices, the in-situ glass sampling method was employed for sample collection (Yang, 2005; Dong *et al*., 2005; Liang *et al*., 2013; Wang *et al*., 2016). Liang *et al*. (2013) and Wang *et al*. (2013a) have shown that increased natural surface roughness (pebbles, gravels, aquatic plants) is associated with biofilm microbial diversity. Accordingly, surfaces of several potential growth matrices in lake water were simulated using glass slides (25 mm × 75 mm) with distinct roughness coefficients (0.1μm, 1.0μm, 10.0μm) for biofilm cultivation. Prior to installation, slides were thoroughly cleaned with deionized water, followed by immersion in a 6:1 H_2O:HNO_3 solution for 24 hours, and finally flushed with deionized water. Cleaned glass slides were fixed on an organic glass shelf (48 cm × 60 cm × 7.5 cm) (Wang *et*

155 *al*., 2016). Overall, 450 glass slides of identical roughness were fixed on each shelf,
156 with three shelves employed (1350 slides) i.e. three shelves of 0.1μm, 1.0μm and
157 10.0μm roughness. Shelves were placed adjacently on the lakebed, 50m from the
158 shore, close to the lake centre, at a depth of 30cm below the water surface.

159 Biofilm cultivation and monitoring took place over a continuous 58-day period,
160 during June and July (Mean Ambient Air Temperature 25^{o}C). Measured solid
161 particulate masses after 58 days of growth were approximately equal to those
162 recorded after 51 days, thus it was considered that biofilms had reached a steady state
163 and the experiment was concluded.

164 There were a total of ten sampling events during the growth period; these
165 occurred at 5-day intervals for the first 6 sample events and at 7-day intervals for the
166 remaining 4 sample events. This sample regime was designed based upon findings
167 from a recent study at Olympic Lake (Wang *et al*., 2016) during which rapid biofilm
168 growth was followed by significantly reduced growth rates; thus it was considered
169 preferable to include higher resolution sampling during the rapid growth phase.
170 Sample events comprised extraction of 45 slides from each shelf (n = 135), with 50%
171 of extracted slides immediately refrigerated at 4°C. Remaining slides were sonicated
172 in a cavitational ultrasonic cleaner (45 min; 40 KHz) for biofilm removal and
173 production of a suspension for analyses.

174

175 ***2.3 Biofilm Constituent Analyses***

176 *2.3.1 Solid (Dry Mass) Particulate Mass*

177 Refrigerated glass slides were dried (vacuum oven at 70°C) to a constant
178 (recorded) weight and then sonicated (45 min; 40 KHz). After washing with deionized
179 water and air-drying, slides were dried and reweighed (recorded), with the difference
180 between the two recorded weights considered to equate to the solid particulate biofilm
181 weight. Five replicates were analyzed for each sample event and roughness coefficient,
182 with mean particulates masses recorded and employed for modelling.

183

184 *2.3.2. Extracellular Polymeric Substances*

185 Prepared biofilm suspensions were centrifuged (x2000g, 4°C, 15 mins), followed
186 by resuspension of resulting biofilm sediments in a pH 7.0 buffer (Na_3PO_4 2 mmol/L,
187 NaCI 9 mmol/L, NaH_2PO_4 4 mmol/L, and KCl 1 mmol/L) and heated to 80°C for 1 h.
188 Subsequently, samples were centrifuged (x12,000g, 4°C, 15 mins) for EPS extraction.
189 The phenol/sulfuric acid method (Nocker *et al*., 2007) and the Lowry method (NaOH)
190 (Lowry *et al*., 1951) were used to quantify extracellular carbohydrate
191 (polysaccharides) content and extracellular protein content, respectively. Both
192 methods are frequently used due to their relative simplicity and sensitivity within
193 normal EPS content ranges.

194

195 *2.3.3. Metal Oxides (Al, Fe, and Mn)*

196 The content of Al, Fe, and Mn oxides were measured in solution using an

197 analogous method to that previously described by Dong *et al*. (2005). Two slides for
198 each matric roughness coefficient were selected after each of the ten sample events (n
199 = 60). Glass slides with attached biofilms were rinsed (ddH_2O) and placed in 100 mm
200 glass petri dishes with 60 ml 15% HNO_3 and shaken for 24h, thus permitting Al, Fe,
201 and Mn oxide solute extraction. Acidified solute extracts of Fe and Mn were analyzed
202 via flame atomic absorption spectroscopy (FAAS) (WYX-9004; Shenyang, China),
203 with Al extractions analyzed by internally coupled plasma atomic emission
204 spectroscopy (ICP-AES) (PE-1000; Shenyang, China).
205
206 ***2.4 Nitrogen and Phosphorous Adsorption***
207 An analogous method to that employed by Liu *et al*. (2015) was used to quantify
208 maximum nitrogen and phosphorous adsorption in biofilm samples. Based upon
209 experimental results obtained during the current study (Figures 2, 3 and 5), 25-day
210 samples were employed for these analyses. Summarily, 28 slides representing each
211 roughness coefficient were collected and individually placed in 100 ml centrifuge
212 tubes, followed by addition of increasing NH_4Cl concentrations (0, 5, 10, 15, 20, 25,
213 30 mg/l) and the same concentration gradient of KH_2PO_4 to a final volume of 55 ml (n
214 = 84). Samples were stored at 25°C for 24 hours, centrifuged (x2000g, 4°C, 10 mins),
215 and filtered through a 0.45μm membrane. Concentrations of ammonium nitrogen and
216 phosphate in solution were measured via ISC1500 ion chromatography. The quantity
217 of ammonium nitrogen and phosphate adsorbed by the biofilm were calculated via
218 subtraction of the relevant NH_4Cl and KH_2PO_4 concentrations. The *Linear*,

Freundlich and *Langmuir* isotherm equations (Headley *et al*., 1998) were employed for biofilm adsorption isotherm fitting, in addition to the analytical isotherms of nitrogen and phosphorus.

2.5 Modelling Biofilm Growth Kinetics

The biofilm growth process is typically divided into four phases after initial attachment, namely, the adaptive, growth, stable, and shedding phases, with biofilm growth equal to the difference between net growth and shedding (Taylor & Jaffe, 1990). Accordingly, based upon previous studies, the following assumptions were made: (1) biofilm net growth (Y_1), conformed to the logistic growth model (Richards *et al*. 1959), (2) maximum biofilm shedding is equal to maximum growth minus the final biofilm quantity (Pizarro *et al*., 2014) and (3) net biofilm growth exhibits a linear correlation with matrix roughness (R); thus the stable biofilm volume will also exhibit a linear correlation with R (Gjaltema *et al*., 1994). Based upon assumption (1), net biofilm growth (Y_1), is described by (Eqn. 1):

$$Y_1 = \frac{y_{max}}{1 + b_1 \times e^{-b_2 \times T}} \quad \text{(Eqn. 1)}$$

Accordingly, biofilm shedding quantity (Y_2), is obtained by (Eqn. 2),

$$Y_2 = b_3 \times \left(\frac{y_{max} - y_{(T\to\infty)}}{1 + b_1 \times e^{-b_2 \times T}}\right)^{b_4} \quad \text{(Eqn. 2)}$$

Based upon assumption (3) (net biofilm growth exhibits a linear correlation with matrix roughness), net growth quantity (Y_1) and shedding volume (Y_2) were amended as follows:

$$Y_1 = b_5 \times R \times \left(\frac{y_{max}}{1 + b_1 \times e^{-b_2 \times T}}\right) \quad \text{(Eqn. 3)}$$

$$Y_2 = b_3 \times \left(b_5 \times R \times \left(\frac{y_{max} + n \times R \times y_{(T\to\infty)}}{1 + b_1 \times e^{-b_2 \times T}}\right)\right)^{b_4} \quad \text{(Eqn. 4)}$$

Growth quantity (Y) is equal to the difference between net growth and shedding quantity (Eqn. 5):

$$Y = Y_1 - Y_2 = b_5 \times R \times \left(\frac{y_{max}}{1 + b_1 \times e^{-b_2 \times T}}\right) - b_3 \times \left(b_5 \times R \times \left(\frac{y_{max} + n \times R \times y_{(T\to\infty)}}{1 + b_1 \times e^{-b_2 \times T}}\right)\right)^{b_4} \quad \text{(Eqn. 5)}$$

Figure 1 presents a graphical representation of the biofilm growth kinetic model employed in the current study. In *Eqns* 1 – 5, Y represents the unit-area of each biofilm constituent; Y_1 is net growth (unit-area) of each biofilm constituent; Y_2 is the measured shedding quantity (unit-area) of each biofilm constituent; R is the matrix roughness; y_{max} is the maximum measured quantity (unit-area) of each biofilm constituent; $y_{(T\to\infty)}$ is the unit-area of each biofilm constituent based upon an infinite

growth period; T is the biofilm growth period; b_1, b_2, b_3, and b_4 are equation parameters; n, and b_5 are roughness parameters.

The Levenberg-Marquardt (LM) algorithm, an iterative numeric minimization algorithm for solving non-linear least squares problems, was used to fit the non-linear relationship between measured solid particulate mass and biofilm growth time. The optimization software package *1stOpt* was use to iteratively run the LM algorithm and generate statistical test parameters for all developed models (RMSE, DC, R, R^2, χ^2, F). The generated F-statistic was used to adjudge model fitting accuracy; based upon employed degrees of freedom (*df* = 9) and critical value tables, a critical F-statistic value of 5.1 was employed.

3. Results

3.1 Solid Particulates and Biofilm Growth

Temporal variation associated with measured solid particulate mass per unit area during the experimental period is presented in Figure 2; as shown, biofilm growth typically adhered to a bacterial growth/kinetic curve, with the overall growth process approximately divided into three phases, namely rapid growth, rapid shedding, and dynamic stability. A relatively rapid and stable solid particulate mass increase conforming to an exponential curve was exhibited from 0–30 days (growth phase) among all three growth matrices (0.1µm, 1.0 µm and 10.0 µm), with maximum values of 3.32, 3.54, and 4.22 mg cm^{-2}, respectively. Thus, growth matrix surface roughness was found to directly correlate with measured solid particulate mass (R^2 = 0.85 - 0.96).

A logarithmic particulate mass decrease was noted during the 30-50 day period (rapid shedding), with the aforementioned correlation remaining in place after 50-day growth. After 50 days, all three matrices entered a stationary growth phase, during which the measured biofilm mass associated with the 1.0-μm roughness matrix was greatest (1.80 mg cm^{-2}), while that of the 0.1-μm and 10-μm roughness matrices exhibited a similar solid particulate mass (≈1.2 mg cm^{-2}).

Growth model parameters based upon results of LM iterative modelling are presented in Table 2. As shown, non-linear correlations indicate an appropriately accurate model fit (R^2 = 0.79 – 0.95), with the F-statistic significantly greater than the calculated critical value (F >5.1) (i.e. appropriately accurate fitting function).

3.2 Extracellular Polymeric Substances and Biofilm Growth

Temporal variation associated with measured contents of extracellular proteins, extracellular polysaccharides and total extracellular polymeric substances (EPS) are presented in Figure 3. As shown, in all cases the measured mass of extracellular protein, extracellular polysaccharide and EPS adhered to a bacterial growth/kinetic curve over the duration of biofilm growth. As for solid particulates, the growth process could be approximately divided into three distinct periods; rapid growth, rapid shedding, and dynamic stability. During the first phase (0–30 days), contents of extracellular proteins, extracellular polysaccharides and EPS increased quickly to their maximum values on all growth matrices. Maximum values for all three measured extracellular constituents were exhibited by biofilms cultivated on the

10-μm matrix (0.17 mg cm^{-2} extracellular proteins, 0.70 mg cm^{-2} extracellular polysaccharides, and 0.88 mg cm^{-2} EPS), with lowest maximum values observed on the 0.1-μm matrix (0.13 mg cm^{-2} extracellular proteins, 0.38 mg cm^{-2} extracellular polysaccharides, and 0.53 mg cm^{-2} EPS).

During the shedding phase (30–50 days), measured constituent volumes decreased rapidly, with stabilization occurring from approximately day-50 (i.e. initiation of stationary phase). During the stationary phase, measured constituent volumes were greatest in biofilms grown on the 1.0-μm roughness matrix (0.05 mg cm^{-2} extracellular proteins, 0.16 mg cm^{-2} extracellular polysaccharides, and 0.26 mg cm^{-2} EPS), with lowest measured values associated with the 0.1-μm matrix (0.04 mg cm^{-2} extracellular proteins, 0.10 mg cm^{-2} extracellular polysaccharides, and 0.17 mg cm^{-2} EPS).

Nonlinear fitting of the relationship between measured EPS and biofilm growth was undertaken using the LM algorithm. As shown (Table 3), all calculated R^2 values were ≥ 0.7 (0.7 – 0.99), with all F-values significantly greater than 5.1, thus indicating a good model fit.

3.3 Metal Oxides and Biofilm Growth

Al, Fe, and Mn oxides followed a bacterial growth curve during biofilm growth, thus exhibiting similar patterns to those of measured solid particulates and EPS (Figure 5). During all phases of biofilm growth, the order of measured oxides followed Fe>Al> Mn; maximum values were observed after 30 days on biofilms

associated with a surface roughness of 10μm (45.92 μg/cm^2, 39.68μg/cm^2, 3.44 μg/cm^2), with minimum values observed on surfaces with a 0.1μm roughness coefficient (35.84 μg/cm^2, 28.56 μg/cm^2, 2.43 μg/cm^2). During the stationary phase, oxides were highest in biofilms formed on surfaces with a roughness of 1.0μm (17.40 μg/cm^2, 14.00 μg/cm^2, 1.38 μg/cm^2), with lowest levels observed in those formed on surfaces with a roughness of 10μm (12.70 μg/cm^2, 11.30 μg/cm^2, 0.87 μg/cm^2). As for EPS, nonlinear fitting of the relationship between metal oxides and biofilm growth was successfully achieved using the LM algorithm (Table 4); calculated R^2 values were ≥ 083 (0.83 – 0.97), with all F-values significantly greater than 5.1 (F = 46 - 330).

3.3 Nutrient Adsorption Characteristics and Modelling

Measured biofilm N/P isotherms and unit contents of biofilm constituents after 25d growth are presented in Figure 5 and Table 5, respectively, with results of *Linear*, *Freundlich,* and *Langmuir* isotherm modelling outlined in Table 6. Ammonium nitrogen and phosphorus concentrations adhered to an expected trend i.e. adsorption capacity increased in concurrence with increasing solution equilibrium concentration (Fig. 4). Biofilm adsorption of both ammonium nitrogen and phosphorus were notably lower in background solutions of reclaimed water than ddH_2O (Fig. 4). All three models for ammonium nitrogen and phosphorus adsorption exhibited high levels of validation (R^2 ≥ 0.91). Within ammonium nitrogen models, fitting parameters Kd (sorption coefficient), Sm (saturated maximum adsorption capacity), and MBC

348 (maximum buffering capacity) were all shown to increase in concurrence with an
349 increased matrix roughness coefficient in both background solutions (reclaimed water
350 and ddH_2O). In the case of deionized water, the order of 1/n (slope of adsorption
351 isotherm i.e. adsorption stability) was $1/n_{1.0} > 1/n_{0.1} > 1/n_{10.0}$, while this was $1/n_{0.1} >$
352 $1/n_{1.0} > 1/n_{10.0}$ for reclaimed water. Within phosphorus models, the order of Kd was
353 $Kd_{10} > Kd_{0.1} > Kd_{1.0}$, while the order of S_m was $Sm_{0.1} > Sm_{10.0} > Sm_{1.0}$ for both
354 background solutions. Significantly different phosphorus modelling results were
355 found between the background solutions for both 1/n and MBC; orders of $1/n_{1.0} >$
356 $1/n_{10.0} > 1/n_{0.1}$, and $MBC_{0.1} > MBC_{10.0} > MBC_{1.0}$ resulted from ddH_2O, while these
357 were $1/n_{1.0} > 1/n_{0.1} > 1/n_{10.0}$, and $MBC_{10.0} > MBC_{0.1} > MBC_{1.0}$ for reclaimed water. As
358 shown (Table 6), reclaimed water was associated with significantly lower model
359 fitting parameters (Kd, Sm, and MBC) for both ammonium nitrogen and phosphorus
360 i.e. decreased adsorption capacity. Conversely, an increased 1/n was also associated
361 with reclaimed water, irrespective of matrix roughness coefficient.
362
363 **4. Discussion**
364 Biofilm formation and adhesion are significantly associated with numerous
365 factors including hydrological conditions, matrix type, nutrition level, and light, with
366 growth matrix surface roughness recognized as a particularly important variable (Tang
367 *et al*., 2013). Results from the current study show that biofilm growth adheres to a
368 bacterial growth curve (Fig. 2), characterized by rapid growth (0 – 30 days), rapid
369 shedding (30 – 50 days), and dynamic stability (>50 days). These findings are

370 mirrored and substantiated by previous studies which have investigated the condition
371 and duration of biofilm formation in water supply systems and found that biofilms
372 formed a stable microbial community via an
373 attachment-growth-shedding-reattachment cycle (Wimpenny, 1996; Hall-Stoodley *et*
374 *al*., 2004). Typically, during the rapid growth phase, microbial mass and diversity rise
375 quickly, leading to increased EPS secretion, solid particulate adsorption, and
376 subsequent biofilm proliferation. Rapid shedding is characterized by inhibited nutrient
377 transfer and resultant microbial die-off; thus, EPS secretion decreases, leading to a
378 lack of adhesion and subsequent shedding. This is followed by dynamic stability
379 whereby microbial mass and diversity remain relatively constant, with the concurrent
380 processes of new biofilm attachment and mature biofilm exfoliation occurring in
381 relative equilibrium (Hall-Stoodley *et al*., 2004; Lear & Lewis, 2012).

382 Findings from the current study indicate that biofilm growth is represented by a
383 "dynamically balanced" process of growth-shedding-regrowth, which has been
384 appropriately characterized by the established model. The developed model adheres to
385 the assumption that biofilm growth is equal to the difference between net growth and
386 shedding, with this relationship summerised in terms of surface roughness (R) as
387 follows: when $R = 0.1\mu m$, $n > 0$ and when $R \geq 1.0\mu m$, $n \leq 0$; thus, the matrix surface
388 was conducive to biofilm shedding and impeded attachment when $R = 0.1\mu m$.

389 Maximum solid particulate contents of 3.32, 3.54, and 4.22 mg cm^{-2}, were
390 associated with 0.1μm, 1.0μm, and 10.0μm surface roughness coefficients,
391 respectively (Fig. 2). Previous studies of biofilm attachment to aquatic plant and

392 artificial substrate surfaces in Chinese freshwater lakes have reported solid particulate
393 contents occurring within the range 1.5 – 2.9 mg/cm^2 (Yang, 2005; Wang *et al*.,
394 2013a); Yang (2005) has reported mean solid particulate contents of 2.35 mg/cm^2 in
395 biofilms cultivated on glass slides similar to those used in the current study.
396 Accordingly, it may be concluded that biofilms occurring in reclaimed water are
397 associated with elevated solid particulate volumes, with findings from the current
398 study indicating that these may be as much as 50% higher, depending on the biofilm
399 growth matrix. During the active growth phase, measured biofilm constituent contents
400 were found to be greatest in biofilms grown on 10.0μm surface roughness matrices
401 (Figure 3), thus indicating elevated biofilm growth rates, as previously reported by
402 Wang *et al*. (2016). This occurs due to the increasing adhesive capacity of nutrients
403 and microorganisms in concurrence with an increasing effective surface area (Shafagh,
404 1986).

405 Extracellular polymeric proteins were found to represent the primary biofilm
406 constituent; this is significant as EPS composition and quantity have been shown to
407 affect biofilm porosity, diffusivity, adsorption, and microbial metabolism (Vogt *et al*.,
408 2013). Maximum measured extracellular protein, extracellular polysaccharide and
409 total EPS contents of 0.17, 0.70, and 0.88 mg/cm^2 (40, 165, and 208 mg/g as solid
410 particulates), respectively, were found in biofilms from Olympic Lake (Figure 3).
411 Zhang (2010) has previously shown that the content of extracellular polysaccharides
412 in a biofilm reactor initially increase rapidly, followed by a subsequent decrease and
413 stabilization, similar to overall trends found in the current study. Zhang (2010) also

414 reported maximum extracellular polysaccharides occurring within the range 100 – 120
415 mg/g i.e. 37-65% lower than results from the present study. Analogous experiments
416 carried out in a ddH_2O background corresponded with previous studies i.e. measured
417 contents of solid particulates and EPS were significantly higher in reclaimed water.
418 This is primarily due to the significantly elevated (and complex) organic content
419 associated with reclaimed water (Table 1); higher levels of suspended particulate
420 matter and subsequently available nutrients result in proliferation of both microbial
421 mass and diversity within biofilms (Hall-Stoodley *et al*., 2004; Flemming &
422 Wingender, 2010).

423 Several studies have shown that the presence of metal oxides varying trophic
424 levels will significantly influence surface adsorption processes in water and soils
425 (Perret *et al*., 2000; Dong *et al*., 2005; Wei *et al*., 2011; Huang & Liu, 2013).
426 Accordingly, Al, Fe and Mn oxide variations during biofilm growth were investigated;
427 all three adhered to the bacterial growth curve during biofilm cultivation, with an
428 overall pattern similar to that exhibited by measured solid particulate mass (Figure 5).
429 Measured quantities of both EPS and metal oxides were positively correlated with
430 biofilm nutrient adsorption, with results also indicating that biofilm constituents
431 increase in concurrence with increasing growth surface roughness; the highest
432 experimental roughness coefficient (10.0μm) was associated with absorption of
433 significantly larger volumes of organic and inorganic charged colloids. Tsuneda *et al*.
434 (2003) have shown that bacterial cells within biofilm samples are anionic due to the
435 existence of negative charge groups on their surface and elevated numbers of anionic

groups existing within EPS. Thus, in the current study, biofilms favored adsorption of positively charged NH_4^+. Additionally, biofilms also comprise nitrifying and denitrifying bacteria, resulting in both denitrification and dephosphorylation (Paniagua-Michel & Garcia 2003; Wang *et al*., 2016). Finally, it is likely that Fe^{3+} and Al^{3+} present in solution will combine with PO_4^{3-} to form insoluble compounds conducive to phosphorus adsorption (Olivieri *et al*., 2014). Modelling results (Table 6) show that biofilm adsorption of ammonium nitrogen and phosphorus decreased in reclaimed water as characterized by a decrease in the fitting parameters Kd, Sm and MBC; thus, nutrient adsorption by biofilms are adjudged to be ecologically beneficial, adding to the self-purification capacity of the waterbody. The observed increase in nonlinear parameter 1/n (absorption stability) suggests greater fluctuations of the adsorption curve, leading to decreased adsorption stability. This illustrates both inhibition of biofilm nutrient adsorption and a reduction in the stability of the adsorption process due to increased competitive adsorption. Reclaimed water represents a complex mixture of myriad substances, in which elevated concentrations of ions and organic materials compete for ammonium and phosphorus adsorption sites, thus resulting in competitive adsorption (Wang *et al*., 2013b). Further studies are required to further elucidate the inhibitory mechanisms associated with biofilm growth and nutrient adsorption in reclaimed water. Based upon results of the current study, it is concluded that glass slide cultivation of biofilms is an effective approach to biomonitoring urban lakes utilizing reclaimed water, with a cultivation period of approximately 50 days deemed appropriate. Moreover, biofilm growth associated with

458 a growth matric surface roughness of 10μm was fastest and therefore most
459 ecologically sensitive (i.e. conservative biomonitoring approach).

460 It is important to note that, within the context of ecosystem health assessment, the
461 current study comprised some inherent limitations, instead focusing on biofilm
462 growth kinetics in a reclaimed wastewater background. The current study did not
463 include eco-toxicological analyses, and thus only indicative conclusions pertaining to
464 ecological health may be made. Future work should concentrate on biofilm growth
465 kinetics and responses to the presence of ecologically harmful compounds, in addition
466 to human toxins and pathogens including heavy metals, PAHs, urban pesticides, and
467 endocrine disruptors. Additionally, future work is required to improve current
468 understanding of biofilm formation, structure and contaminant purification capacity in
469 order to make further recommendations pertaining to their use in ecological health
470 assessment.

471 **5. Conclusions**

472 The growth characteristics of biofilms on multiple growth matrix surfaces and
473 their effects on nutrient (NH_4-N and P) adsorption were investigated. Results indicate
474 that biofilm constituent concentrations (solid particulates, metal oxides, and EPS)
475 adhere to a bacterial growth curve, thus mirroring measured biofilm growth in
476 reclaimed water. Biofilm solid particulates were significantly greater in biofilms
477 associated with reclaimed water than those cultivated in ddH_2O, irrespective of
478 growth media surface roughness, while quantified biofilm constituents (Al, Mn, and
479 Fe oxides, extracellular proteins, and extracellular polysaccharides) exhibited

maximum values during the rapid growth phase. Measured biofilm constituents (EPS, Metal Oxides) were significantly higher in the reclaimed water background than a natural water background, thus agreeing with previous studies. Accordingly, it is concluded that biofilms may be effective indicators of ecological health in aquatic ecosystems characterized by the presence of reclaimed water i.e. indicators of system capacity to support food production and/or provide water resources for human use. However, significant further work is required to elucidate the association between biofilm presence and associated kinetics, and the human health related contaminants of primary concern e.g. PAHs, urban pesticides, endocrine disruptors, enteric pathogens, etc. Where biofilms are used for ecological biomonitoring, a growth matrix surface roughness of 10.0μm is preferable due to increased biofilm growth rates and subsequently enhanced sensitivity to ecological variations. The developed growth model describes key biofilm constituent kinetics, while also providing information pertaining to biofilm cultivation times for future biomonitoring. Overall, study results show that metal oxides and EPSs are the key substances actively influencing surface adsorption of biofilms in reclaimed water. Comparative experiments indicate that reclaimed water not only inhibits biofilm adsorption of ammonium and phosphorus, but also reduces nitrogen and phosphorus adsorption stability.

Acknowledgements

The authors gratefully acknowledge financial support from the National Natural

Science Fund of China (No. 51321001), the Key Project of the Beijing Eleventh-Five Year Research Program (No. D090409004009004), Department of Water Resources, Social Research Project (No. 201401054), and the Special Fund for Water Conservancy Scientific Research in the Public Interest (No. 201001067). The authors would also like to thank the anonymous reviewers whose insightful comments and recommendations helped to improve the final manuscript.

References

Ancion PY., Lear G., Neale M., Roberts K., Lewis GD. (2014). Using biofilm as a novel approach to assess stormwater treatment efficacy. *Water Research*. **49**: 406-415

Beaudequin D., Harden F., Roiko A., Stratton H., Lemckert C., Mengersen K. (2015). Modelling microbial health risk of wastewater reuse: A systems perspective. *Environ. International*. **84**: 131-141

Beijing Water Authority (2015). Beijing Water Resources Bulletin 2011-2014

Burns A., Ryder DS. (2001). Potential for biofilms as biological indicators in Australian riverine systems. *Ecol. Manag. Restor.* **2**(1): 53–63

Dong D., Yang F., Li Y., Hua X., Lǔ, X., Zhang J. (2005). Adsorption of Pb, Cd to Fe, Mn oxides in natural freshwater surface coatings developed in different seasons. *Journal of Environmental Sciences*. **17**(1): 30-36.

Eppley RW. (1977). The growth and culture of diatoms. In: The Biology of Diatoms; Ed Werner D. Blackwell Scientific Publications, London. pp 24-64

Flemming HC., Wingender J. (2010). The biofilm matrix. *Nat. Rev. Microbiol*. **8**: 623–633

524 Friedler E., Lahav O., Jizhaki H., Lahay T. (2006). Study of urban population attitudes
525 towards various wastewater reuse options: Isreal as a case study. *Jour. Env. Man*. **81**(4):
526 360-370
527 Gan YP., Bai Y. (2010). The advanced treatment and recycling technologies in Sewage
528 treatment plant, China Building Industry Press, **7**(1):198-314
529 Gao Z., Hu Y. (2011). Coping with population growth, climate change, water scarcity and growing
530 food demand in China in the 21st century. In: Brauch, H.G., *et al*. (Eds.), Coping with Global
531 Environmental Change, Disasters and Security. Springer, Berlin, pp. 957–967
532 Ge L., Xie G., Zhang C., Li S., Qi Y., Cao S., He TT. (2011). An evaluation of China's water
533 footprint. *Water Res. Man*. **25**(10): 2633-2647
534 Gjaltema A., Arts PA., Loosdrecht MC., Kuenen JG., Heijnen JJ. (1994). Heterogeneity of
535 biofilms in a rotating annular reactor: occurrence, structure and
536 consequences. *Biotechnology & Bioengineering*. **44**(2): 194-204.
537 Graczyk TK., Lucy FE. (2006). Quality of reclaimed waters: a public health need for source
538 tracking of wastewater-derived protozoan enteropathogens in engineered wetlands. *Trans.*
539 *R. Soc. Trop. Med. Hyg*. **101**(6): 532-533
540 Guasch H., Admiraal W., Sabater S. (2003). Contrasting effects of organic and inorganic
541 toxicants on fresh water periphyton. *Aquatic Toxicology*. **64**: 165-175.
542 Hall-Stoodley L., Costerton JW., Stoodley P. (2004). Bacterial biofilms: from the natural
543 environment to infectious diseases. *Nat Rev Micro*. **2**(2):95–108
544 Headley JV., Gandrass J., Kuballa J., Peru KM., Yiling Gong Y. (1998). Rates of sorption and
545 partitioning of contaminants in river biofilm. *Environ. Sci. Technol*. **32**: 3968–3973

546 Hill BH., Hall RK., Husby P, Herlihy AT., Dunne M. (2000). Interregional comparison of
547 sediment microbial respiration in streams. *Freshwater Biology*. **44**: 213-222.
548 Hong L, Herbert HP. (2002). Extraction of extracurricular polymeric substances (EPS) of
549 sludges. *Journal of Biotechnology*. **95** (3): 249-256.
550 Huang W., Liu ZM. (2013). Biosorption of Cd(II)/Pb(II) from aqueous solution by
551 biosurfactant-producing bacteria: isotherm kinetic characteristic and mechanism studies.
552 *Colloids Surf. B.* **105**: 113–119.
553 Jenerette GD., Wu W., Goldsmith S., Marussich W., Roach WJ. (2006). Contrasting water
554 footprints of cities in China and the United States. *Ecological Economics*. **57**: 346 - 358.
555 Lawrence JR., Chenier MR., Roy R., Beaumier D., Fortin N., Swerhone GD, Neu TR., Greer
556 CW. (2004). Microscale and molecular assessment of impacts of nickel, nutrients, and
557 oxygen level on structure and function of river biofilm communities. *Appl. Environ.*
558 *Micro*. **70**: 4326–4339.
559 Lear G., Lewis GD. (2009). Impact of catchment land use on bacterial communities within
560 stream biofilms. *Ecological Indicators*. **9**: 848-855
561 Lear G., Lewis GD. (2012). Microbial Biofilms: Current Research and Applications. Caister
562 Academic Press. Norfolk. UK.
563 Liang MC., Wang TZ., Li Y., Yang PL., Liu CC., Li PX., Wei Z. (2013). Structural and fractal
564 characteristics of biofilm attached on the surfaces of aquatic plants and gravels in the
565 rivers and lakes reusing reclaimed wastewater. *Environmental Earth Science.* **70**(5):
566 2319-2333.
567 Liu ZW., Li PX., Ning Z., Xiao Y., Wang CZ., Li YK. (2015). A modified attapulgite clay for

controlling infiltration of reclaimed water in a riverbed. *Environmental Earth Sciences*. **73**（7): 3887-3900

Lowry OH., Rosebrough NJ., Farr AL., Randall RJ. (1951). Protein measurement with the Folin phenol reagent. *J Biolol Chem.* **193**(1):265–275

Nocker A., Lepo JE., Martin LL., Snyder RA. (2007). Response of estuarine biofilm microbial community development to changes in dissolved oxygen and nutrient concentrations. *Microbial Ecology*. **54**(3):532-542.

Olivieri A., Seto E., Cooper R., Cahn M., Colford J., Debroux J., Mandrell R., Suslow T., Tchobanoglous G., Hultquist R., Spath D., Mosher J. (2014). Risk-based review of Californias water-recycling criteria for agricultural irrigation. *Jour. Env. Eng*. **140**(6)

Paniagua-Michel J., Garcia O. (2003). Ex-situ bioremediation of shrimp culture effluent using constructed microbial mats. *Aqacultural Engineering*. **28**(3-4): 131-139

Perret D., Gaillard J., Dominik J., Atteia O., (2000). Diversity of natural hydrous iron oxides. *Environ. Sci. Technol*. **34**(17): 3540-3546.

Pizarro G., Griffeath D., Noguera DR. (2014). Quantitative cellular automaton model for biofilms. *Journal of Environmental Engineering.* **127**(9), 782-789.

Porsbring T. (2007). The SWIFT periphyton test for high-capacity assessments of toxicant effects on micro-algal community development. *Journal of Experimental Marine Biology and Ecology*. **349**(2): 299-312

Rao TS. (1997). Biofilm formation in a freshwater environment under photic and aphotic conditions. *Biofouling*, **11**(4): 265-282.

Richards FJ. (1959). A flexible growth function for empirical use. *J. Exp. Botany*. **10**(2)

590 Rotter S., Heilmeier H., Altenburger R., Schmitt-Jansen M. (2013). Multiple stressors in
591 periphyton – comparison of observed and predicted tolerance responses to high ionic loads
592 and herbicide exposure. *Jour. Appl. Ecology*. **50**(6): 1459-1468
593 Shafagh J. (1986). Plaque accumulation of cast gold complete crown. *Prosthet Dent*. **55**:
594 339-342.
595 Tang L., Schramm A., Neu TR., Revsbech NP., Meyer RL. (2013). Extracellular DNA in
596 adhesion and biofilm formation of four environmental isolates: a quantitative study.
597 *FEMS Micro. Ecol*. **86**(3): 394-403
598 Tatlor GT. (1997). Influence of surface properties on accumulation of conditioning flims and
599 marine bacterial on substrata exposed to oligotrophic water. *Biofouling*, **11**(1): 31-57.
600 Taylor SW., Jaffe PR. (1990). Biofilm growth and the related changes in the physical
601 properties of a porous medium : 3. Dispersivity and model verification. *Water Resources*
602 *Research*. **26**(9): 2171-2180
603 Tsuneda S., Aikawa H., Hayashi H., Yuasa A., Hirata, A. (2003). Extracellular polymeric
604 substances responsible for bacterial adhesion onto solid surface. *FEMS Microbiol. Lett*.
605 **223**: 287–292.
606 Vogt SJ., Sanderlin AB., Seymour JD., Codd SL. (2013). Permeability of a growing biofilm in
607 a porous media fluid flow analyzed by magnetic resonance displacement-relaxation
608 correlations. *Biotech. Bioeng*. **10**(5): 1366-1375
609 Wang TZ., Li YK., Liang MC., Yang PL., Bai Z. (2013a). Biofilms on the surface of gravels
610 and aquatic plants in rivers and lakes with reusing reclaimed water. *Environmental Earth*
611 *Sciences*. **72**(3): 743-755.

612 Wang XH., Liu FF., Lu L., Yang S., Zhao Y., Sun LB., Wang SG. (2013b). Individual and
613 competitive adsorption of Cr(VI) and phosphate onto synthetic Fe–Al hydroxides. *Coll. Sur. B.*
614 **423**: 42-49

615 Wang TZ., Li YK., Xu TW., Wu NY., Liang MC., Hynds P. (2016). Biofilm microbial
616 community structure in an urban lake utilizing reclaimed water. *Environmental Earth*
617 *Sciences*. **75**:314

618 Wei X., Fang LC., Cai P. (2011). Influence of extracellular polymeric substances (EPS) on Cd
619 adsorption by bacteria. *Environ. Pollut*. **159**: 1369–1374.

620 Wimpenny J. (1996). Ecological determinants of bioflim formation. *Biofouling*. **10**: 43-63.

621 Yan JX., Liu JL., Ma MY. (2014). In situ variations and relationships of water quality index
622 with periphyton function and diversity metrics in Baiyangdian Lake of China.
623 *Ecotoxicology*. **23**(4): 495-505

624 Yang F. (2005). Growth regularity and adsorption characteristics of important constituents in
625 surface coatings developed in natural waters (Unpublished PhD thesis). Jilin University,
626 Changchun, China

627 Zhang X., 2010. Research of Biofilm Reactor in Moving Bed (Unpublished PhD thesis).
628 Beijing Forestry University, Beijing, China

629 Zhang C., Anadon LD. (2014). A multi-regional input-output analysis of domestic virtual
630 water trade and provincial water footprint in China. *Ecological Economics*. **100**: 159-172

631

632 Zhao X., Chen B., Yang ZF. (2009). National water footprint in an input-output framework – A
633 case study of China 2002. *Ecological Indicators*. **220**(2): 245-253

634

Figure

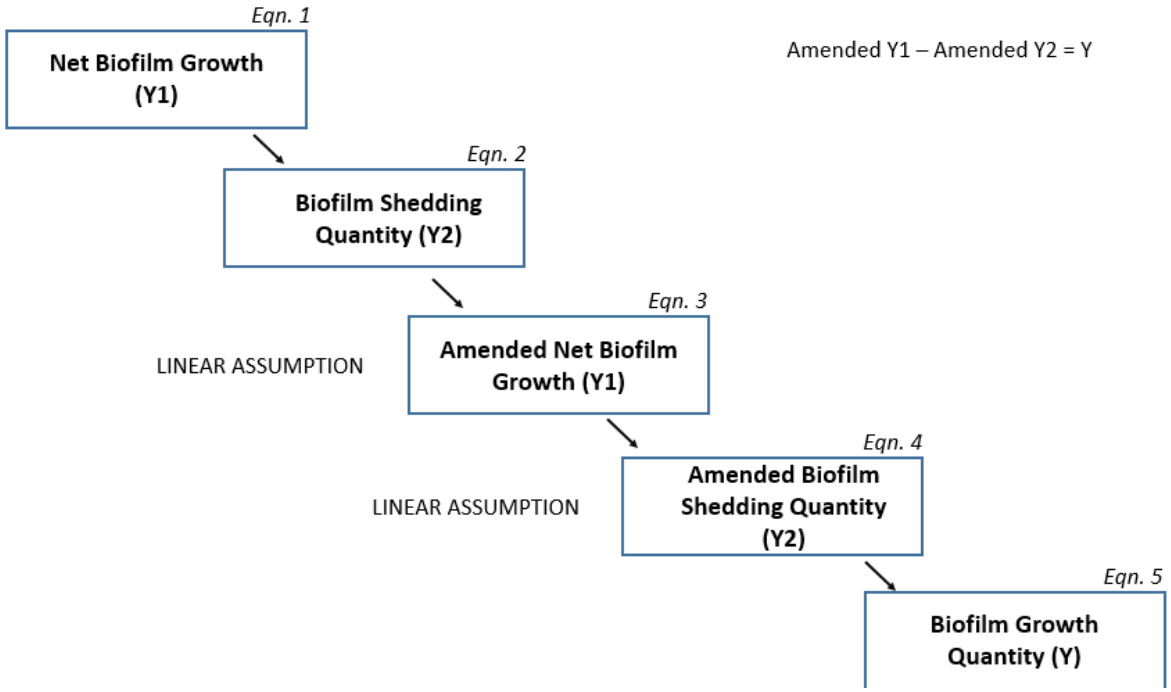

Figure 1. Schematic outlining the employed biofilm growth kinetic model

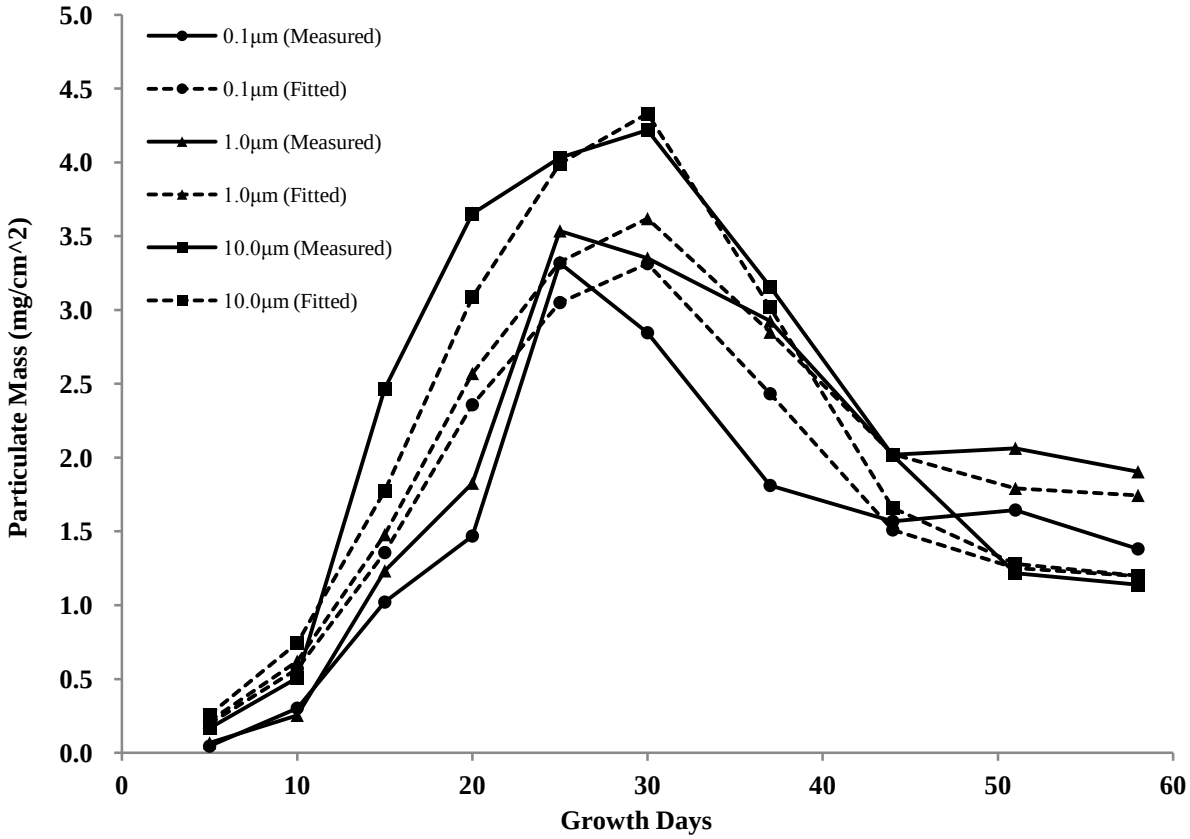

Figure 2. Measured and fitted (Solid particulate mass growth model) solid particulate mass per unit area during 58-day biofilm growth

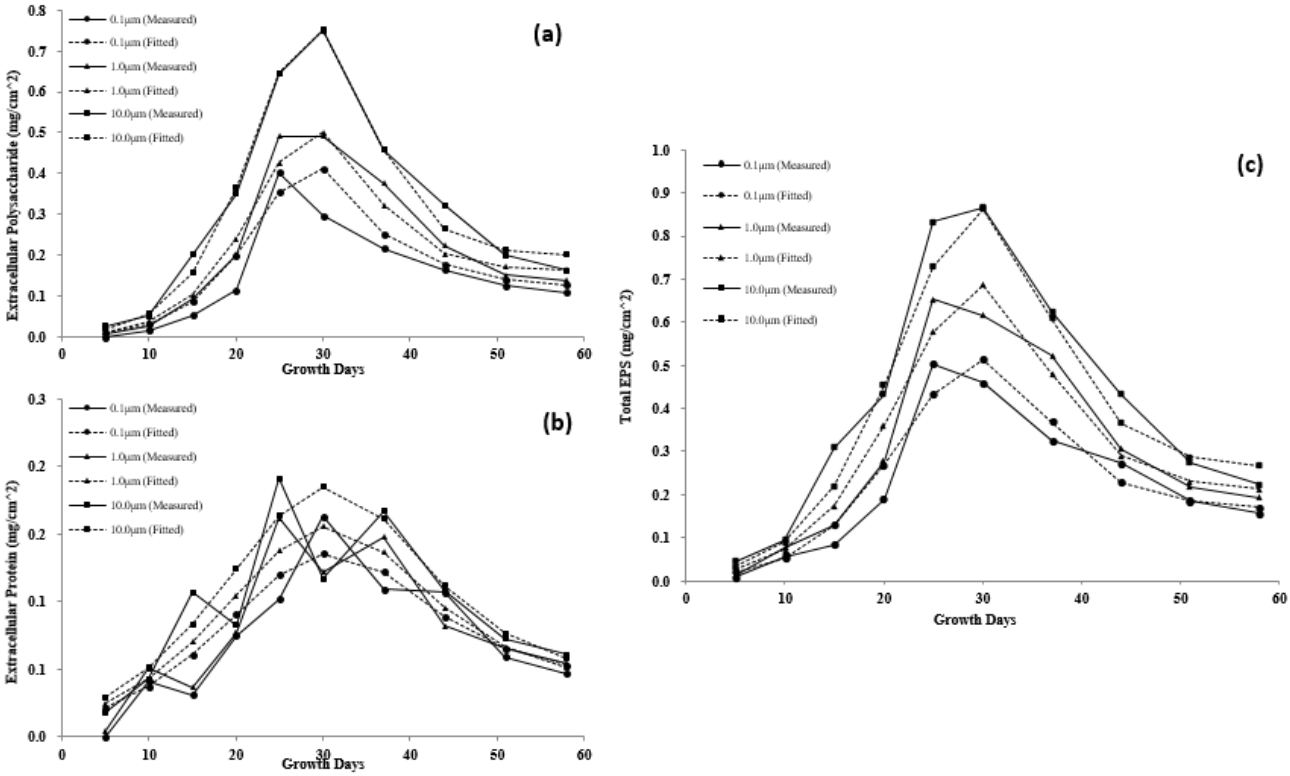

Figure 3. **Measured and fitted (growth models) (a) extracellular polysaccharide, (b) extracellular protein, and (c) total EPS contents per unit area during 58-day biofilm growth**

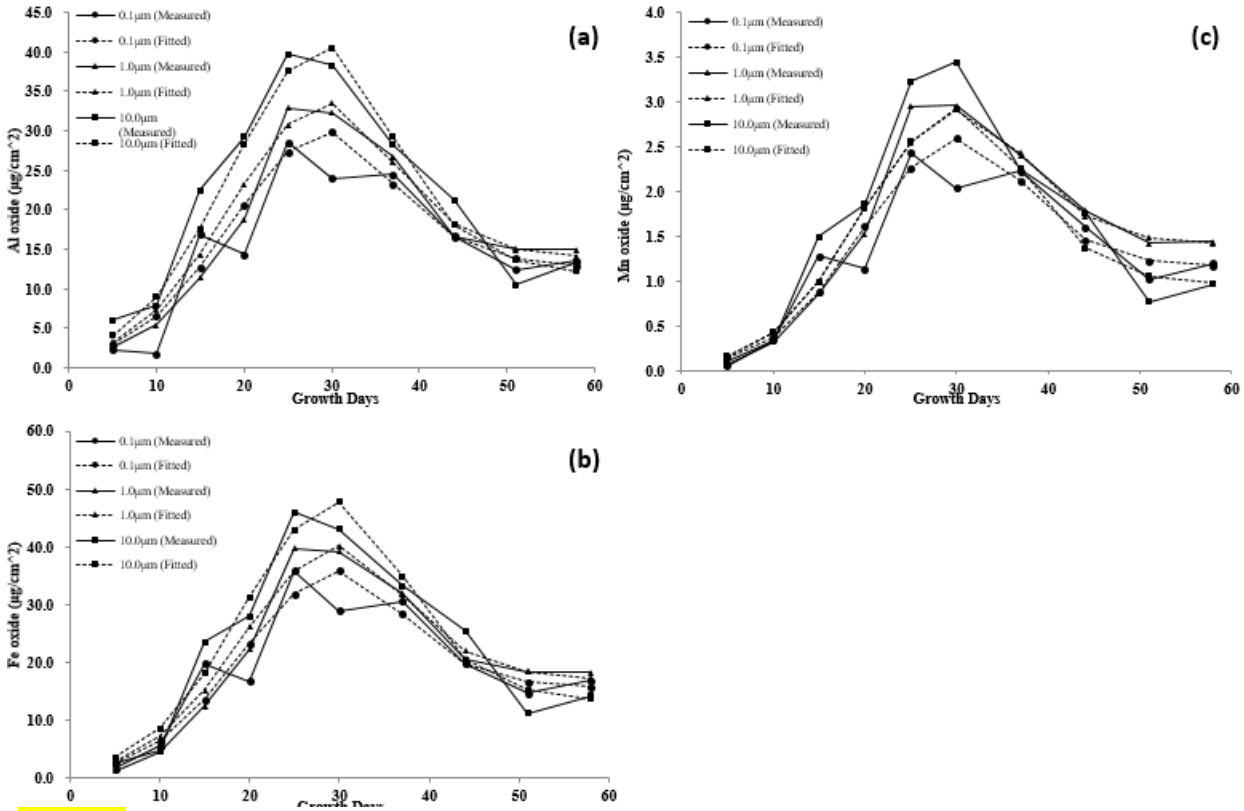

Figure 4. **Measured and fitted (growth models) (a) Al oxide, (b) Fe oxide, and (c) Mn oxide contents per unit area during 58-day biofilm growth**

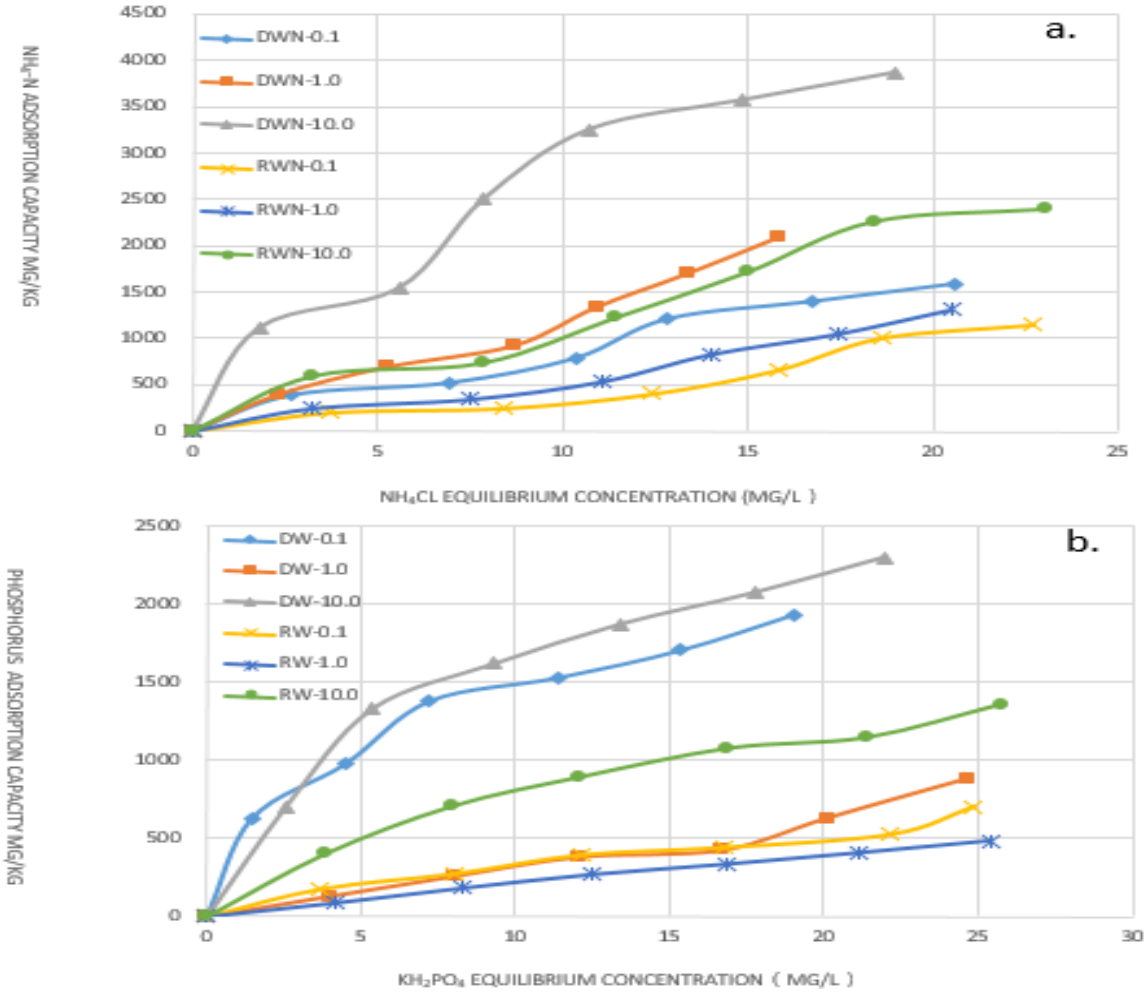

Figure 5. Biofilm adsorption isotherms and analytical isotherms of NH_4-N (a) and P (b) (DW, ddH_2O; RW, reclaimed water)

Table

Time d	T °C	pH	NH_4^+ mg/L	NO_3^- mg/L	TN mg/L	TP mg/L	COD_{Cr} mg/L	BOD mg/L	DO mg/L	Ca mg/L	Mg mg/L
5	25	7.22	5.4	5.92	12.3	0.02	14.2	6.3	6.74	42	26.8
10	26	7.42	7.2	4.78	13.8	0.03	30.2	6.6	7.22	40.1	27.6
15	26	7.38	12.9	3.67	17.1	0.03	29	6.2	5.78	36.5	27.9
20	26	7.29	18.2	2.27	22.8	0.01	28.6	6	4.42	34.2	27.3
25	30	7.97	0.128	0.94	6.24	0.09	12.5	6.9	6.9	41.5	29.6
30	32	7.97	0.432	1.86	6.78	0.09	17.5	2.4	6.83	39.8	29.6
37	30	8.00	0.776	0.37	5.72	0.16	16.2	3.4	6.96	40.4	27.2
44	33	8.13	0.668	1.12	8	0.06	2.1	10.1	6.92	38.3	25.2
51	33	8.20	0.372	2.19	6.63	0.12	11.7	2.4	6.82	38.3	25.2
58	29	8.19	0.608	2.74	12	0.1	8.1	1.6	7.14	40.4	25.2

Table 1. Measured lakewater chemistry during 58-day biofilm cultivation period

Table 2. Solid particulate mass growth model parameters based upon results of Levenberg-Marquardt iterative modelling (*1st Opt*)

Y \ P	R (μm)	b_1	b_2	b_3	b_4	b_5	n	R^2	F
Y_g	0.1	55	0.24	1.2×10^{-51}	91	10.60	1.67	0.79	49
	1.0	55				1.08	−0.13	0.91	108
	10.0	55				0.11	−0.09	0.95	193

Note: Y_g, weights of solid particulates per unit area; R, roughness; R^2, decisive coefficient of fitting function.

Table 3. Extracellular Polymeric Substance (EPS) growth model parameters based upon results of Levenberg-Marquardt iterative modelling (*1st Opt*)

P / Y	R/μm	b_1	b_2	b_3	b_4	b_5	n	R^2	F
	0.1					11.80	0	0.84	57
Y_{pro}	1.0	15	0.13	1.1×10^{6}	10	1.37	−0.33	0.80	40
	10.0					0.14	−0.08	0.70	22
	0.1					14.30	10.00	0.82	52
Y_{pol}	1.0	161	0.22	1.2×10^{1}	11	1.41	0.25	0.96	263
	10.0					0.14	-0.12	0.99	573
	0.1					12.90	10.00	0.92	98
Y_{tEPS}	1.0	90	0.21	0.6×10^{1}	16	1.33	0	0.95	167
	10.0					0.123	−0.08	0.96	271

Note: $Y_{pro,}$ weights of extracellular proteins per unit area; Y_{pol}, weights of extracellular polysaccharides per unit area; Y_{tEPS}, weights of total EPS per unit area; R, roughness; R^2, decisive coefficient of fitting function.

Table 4. Metal oxide growth model parameters based upon results of Levenberg-Marquardt iterative modelling (*1st Opt*)

P / Y	R/μm	b_1	b_2	b_3	b_4	b_5	n	R^2	F
	0.1					12.30	2.50	0.83	46
Y_{Al}	1.0	27	0.18	1.3×10^{-36}	23	1.21	0	0.96	231
	10.0					0.12	−0.05	0.95	183
	0.1					11.80	2.50	0.85	51
Y_{Mn}	1.0	56	0.21	1.8×10^{-23}	45	1.09	0	0.97	317
	10.0					0.11	−0.05	0.90	137
	0.1					11.40	2.50	0.85	47
Y_{Fe}	1.0	39	0.20	2.1×10^{-50}	31	1.15	0	0.97	330
	10.0					0.12	−0.05	0.94	120

Note: Y_{Al}, weights of Al oxide per unit area; Y_{Mn}, weights of Mn oxide per unit area; Y_{Fe}, weights of Fe oxide per unit area; R, roughness; R^2, decisive coefficient of fitting function.

Table 5. Measured unit contents of EPS and metal oxides on day-25 (mg/g)

Constituent / R/μm	Al oxide	Mn oxide	Fe oxide	Extracellular proteins	Extracellular polysaccharides	Total EPS
0.1 μm	8.6	0.7	10.8	30.9	121.0	151.9
1.0 μm	9.3	0.8	11.2	45.7	138.8	184.5
10 μm	9.8	0.8	11.4	47.5	159.4	206.9

Table 6. Validation (Fitting) results of *Linear, Freundlich,* and *Langmuir* isotherm modelling nitrogen and phosphorus adsorption isotherms and change rate of fitting parameters

N/P	Background		Linear				Freundlich				Langmuir				
			a	Kd	Δ	R^2	1/n	Δ	LnK	R^2	Sm	Δ	MBC	Δ	R^2
NH_4^+	0.1 μm	DW	156.22	73.34	-24.9	0.96	0.73	36.3	5.12	0.92	2000	-16.7	172.41	-67.7	0.93
		RW	-138.49	55.06		0.92	1.00		3.69	0.91	1667		55.56		0.91
	1.0 m	DW	-102.79	132.91	-51.9	0.96	0.89	4.5	5.04	0.90	2500	-20.0	188.68	-57.2	0.93
		RW	-68.54	63.89		0.96	0.93		4.23	0.92	2000		80.65		0.95
	10 μm	DW	931.41	171.44	-39.4	0.92	0.57	36.3	6.60	0.93	5000	-33.3	769.23	-72.9	0.94
		RW	124.37	103.86		0.95	0.78		5.30	0.91	3333		208.33		0.91
PO_4^{3-}	0.1 μm	DW	673.86	69.57	-68.2	0.94	0.44	55.7	6.28	0.98	2000	-54.6	625	-90.9	0.96
		RW	95.00	22.12		0.96	0.68		4.25	0.97	909		57.14		0.97
	1.0 m	DW	-34.91	34.11	-45.7	0.95	0.92	1.1	3.62	0.96	10000	-50.1	33.22	-35.7	0.98
		RW	21.34	18.509		0.99	0.93		3.18	0.99	5000		21.36		0.99
	10 μm	DW	775.50	74.39	-45.6	0.92	0.52	19.2	6.17	0.96	3333	-40.0	357.14	-63.6	0.99
		RW	336.68	40.47		0.96	0.62		5.22	0.99	2000		129.87		0.99

Note: DW, deionized water; RW, reclaimed